Contrail Observation and Detection using Ground-Based Cameras

Minh-Thi Bui[1], Dinh-Nam Mai[1]

[1]*Students at National Institute of Applied Sciences of Toulouse, France*

Advisor: Tanguy Chauvet [2]

[2]*Research CLOUD project Product Owner at SII, France*

January 22, 2025

Contents

1 Introduction

The growing concern about aviation's impact on the environment has brought attention to emissions beyond CO_2, especially contrails. Contrails, or condensation trails, are artificial clouds created when aircraft exhaust gas mixes with cold, humid air at high altitudes. These trails can persist for hours and affect the Earth's temperature balance, contributing significantly to global warming. Research shows that 80% of contrail clouds originate from only 5% of flights (Lee et al., 2021), demonstrating the large climate effect caused by a small subset of flights. Understanding how contrails form and their impacts is crucial for developing strategies to reduce their harm.

The European Commission now treats non-CO_2 emissions as seriously as CO_2 emissions, highlighting the need for better monitoring and innovative solutions. According to Lee et al., 2021, non-CO_2 effects contribute approximately 66% of aviation's total radiative forcing impact. To reduce climate impact, the aviation sector must address both CO_2 and non-CO_2, especially persistent contrails, which significantly influence climate. Ground-based observation of contrails is a practical way to collect detailed data on their formation, persistence, and interaction with the atmosphere.

Despite their importance, traditional methods for contrail observation face notable challenges. Satellite imaging, for example, often struggles to reliably link observed contrails to specific flights due to uncertainties in tracking flight paths and atmospheric conditions. While ground-based observation systems exist, they are usually expensive and limited to small, specific areas. These constraints highlight the need for more accessible, low-cost, and scalable solutions.

This project introduces a step-by-step approach for ground-based contrail observation and detection. By optimizing the placement of observation sites, the project ensures effective coverage of high-altitude contrails. The methodology begins with capturing contrail images from fixed setups and calculating the GPS coordinates of the contrail using camera calibration techniques and geospatial data. Advanced computer vision techniques, such as object detection models like YOLO (You Only Look Once), are used to detect and classify contrails based on their characteristics. This approach offers a practical and scalable solution for monitoring contrails, contributing to efforts to reduce aviation's climate impact.

2 Methods

2.1 Determine the Camera's Coverage Area

To determine the camera's observable area, the following steps are performed. First, use the Compass application to determine the phone's central orientation. Next, calculate the camera's field of view (FOV) and the maximum observable distance at the current location. Based on these parameters, the camera's coverage area can be identified, ensuring proper tracking of contrails within the frame.

Procedure for Using a Compass and Capturing Sky Photographs

The first step is to determine the direction before positioning the phone. The phone should be placed parallel to the ground to ensure accurate directional measurements. Once the central direction has been identified, the phone can be adjusted to the appropriate angle for sky photography. A slight tilt may be required to include the entire horizon within the frame.

Using the compass while the phone is held upright is avoided for several reasons. Magnetic field sensors tend to produce unreliable readings in the vertical orientation due to interference from nearby magnetic sources. Such inaccuracies can lead to skewed results, particularly affecting the precision of boundary angle measurements.

Field of View (FOV) Calculation

The field of view (or angle of coverage) can be calculated from the sensor size and focal length using the equation described in Figure 1:

$$\text{FOV} = 2 \cdot \arctan\left(\frac{\text{sensor size}}{2 \cdot \text{focal length}}\right) \tag{1}$$

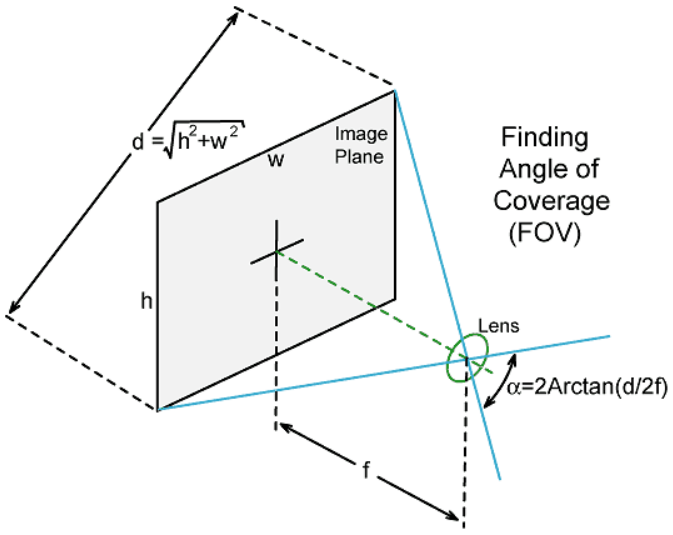

Figure 1: Illustration of the field of view calculation. Image source: Knight, 2018

Depending on the dimension of interest, the respective fields of view can be expressed as follows:

Horizontal FOV (hFOV):

$$\text{hFOV} = 2 \cdot \arctan\left(\frac{\text{Sensor width}}{2 \cdot \text{focal length}}\right) \tag{2}$$

Vertical FOV (vFOV):

$$\text{vFOV} = 2 \cdot \arctan\left(\frac{\text{Sensor height}}{2 \cdot \text{focal length}}\right) \tag{3}$$

Diagonal FOV (dFOV):

$$\text{dFOV} = 2 \cdot \arctan\left(\frac{\text{Sensor diagonal}}{2 \cdot \text{focal length}}\right) \tag{4}$$

When the camera uses a 16:9 aspect ratio in video mode, the image is cropped from its native 4:3 (16:12) format. As a result, the horizontal field of view decreases while the vertical field of view remains unchanged. In this scenario, the diagonal field of view can be expressed as:

$$\text{dFOV} = 2 \times \arctan\left(\frac{\sqrt{(\text{Sensor Width})^2 + (\text{Sensor Height})^2}}{2 \times \text{Focal Length}}\right) \tag{5}$$

Maximum Observable Distance

Assume the Earth is a sphere with radius R. Observations are performed from a point at height h above the surface. The horizon is defined as the intersection of the observer's line of sight with the Earth's surface.

From the Pythagorean theorem:

$$(R + h)^2 = R^2 + D^2 \tag{6}$$

Since $h \ll R$, we approximate $R + h \approx R$. Hence,

$$D \approx \sqrt{2\,R\,h} \tag{7}$$

Calculating Boundary Coordinates

To determine the observable region on Earth's surface, begin by calculating the boundary angles based on the camera's central orientation and horizontal field of view. These angles define the left and right limits of the viewing area. Next, use these angles to find the corresponding latitude and longitude offsets, providing an accurate representation of the camera's coverage.

- Boundary Angles
  - Central orientation θ_c (measured by the compass): Choosing the observation direction to be perpendicular to the flight path helps maximize contrail visibility.
  - Left boundary angle:

$$\theta_{\text{left}} = \theta_c - \frac{\text{hFOV}}{2} \tag{8}$$

- Right boundary angle:

$$\theta_{\text{right}} = \theta_c + \frac{\text{hFOV}}{2} \tag{9}$$

- Coordinate Computation
  - Latitude change:

$$\Delta\text{lat} = \frac{D}{R}\cos(\theta) \tag{10}$$

  - Longitude change:

$$\Delta\text{lon} = \frac{D}{R\cos(\text{latitude})}\sin(\theta) \tag{11}$$

  where:

  - D: Maximum observation distance (in meters).
  - R: Earth's radius (6,371,000 m).
  - θ: Boundary angle (left or right)
  - *latitude*: Current latitude of the camera.

  After computing the changes in latitude and longitude for both the left and right boundaries relative to the current position, the resulting offsets can be added to the current GPS coordinates. This provides the precise boundary coordinates for the observation region.

2.2 Propose Optimal Distance between two Cameras

Using a single camera is infeasible for determining contrail coordinates based solely on its captured images. Consequently, a second camera is placed along the first camera's central axis but oriented in the opposite direction. By combining simultaneous images from both cameras, it becomes possible to calculate the coordinates of the contrails and the aircraft. This section addresses the problem of determining the proposed optimal distance between the two cameras.

Problem Modeling

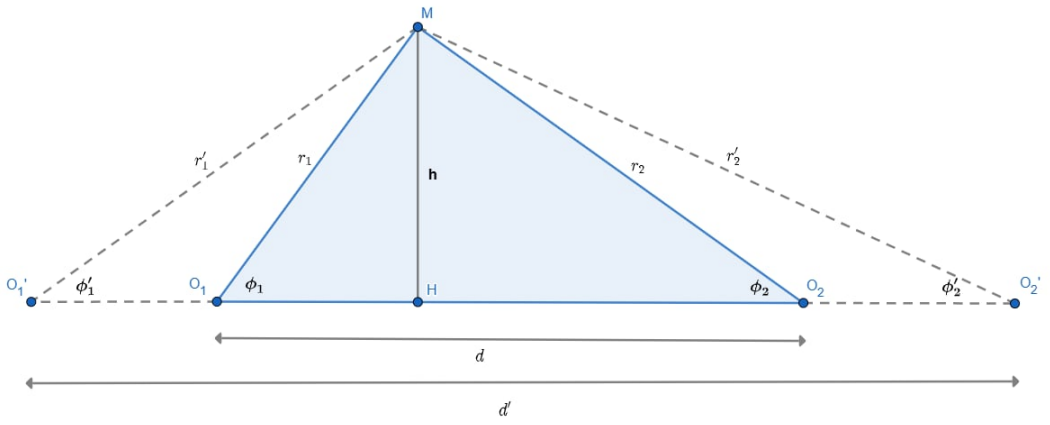

Figure 2: Modeling the problem of determining the optimal distance between two cameras

In this problem, we consider three main points: the positions of the two cameras, denoted as O_1 and O_2, and the contrail position, denoted as M (see Figure 2). The objective is to determine the optimal distance between the two cameras allowing efficient observation and accurate calculation of the contrail's position.

We introduce the following notation:

- d: distance between two cameras (O_1O_2)
- h: contrails altitude
- r_1, r_2: distances from each camera to the contrail
- ϕ_1, ϕ_2: angles between the line connecting each camera to the contrail and the horizontal plane
- The prime symbol (') indicates different values corresponding to another set of positions O_1' and O_2'.

Variables Analysis

Angles ϕ_1, ϕ_2: To simplify the analysis, we assume $\phi_1 = \phi_2 = \phi$. This assumption is reasonable, as any discrepancy between ϕ_1 and ϕ_2 can be corrected by adjusting the position of the second camera to increase ϕ_2, thereby reducing the distance between the cameras.

Contrail altitude h: Contrails are typically formed at altitudes ranging from 8 km to 12 km. For this analysis, we assume $h = h_{\max} = 12$ km to ensure that the distance between the two cameras allows for the observation of most contrails. Indeed, if contrails at this altitude can be observed clearly, contrails at lower altitudes will also be observable. Therefore, the problem of determining the optimal distance d between the two cameras is reduced to finding the optimal angle ϕ.

Effect of angle ϕ on Contrail Pixel Display: The distance from the camera to the contrail r is calculated based on the contrail's altitude h and the angle ϕ using the formula:

$$r = \frac{h}{\sin(\phi)} \tag{12}$$

where h represents the maximum altitude, as mentioned above, to account for the most challenging scenario.

As the distance r between a camera and the contrail increases, the apparent size of the contrails decreases, reducing the number of pixels p representing the contrails in the image. The relationships between p and r is given by:

$$p = \frac{w}{r} \cdot \frac{R}{2\tan\left(\frac{\text{vFOV}}{2}\right)} \tag{13}$$

where:

- w is the contrail width. For this analysis, we assume $w = 200$ m, the typical minimum value reported by the Federal Aviation Administration (FAA, 2000), to examine the most challenging scenario where contrails are the least spread out.

- R is the vertical resolution of the camera
- vFOV is the camera's vertical field of view

To enhance the clarity of contrails in the image, it is necessary to increase ϕ. By doing so, the distance r decreases, leading to an increase in the number of pixels representing the contrails.

Effect of ϕ on Height Calculation Accuracy In the previous analyses, the maximum value of h was considered; however, this assumption is not always applicable. In practice, the contrail altitude h must be calculated based on the distance between the two cameras, d, and other parameters. An essential factor to address is the accuracy of these calculations.

The contrail altitude h is influenced by the angle ϕ and the camera distance d, as expressed by the following relationship:

$$h = \frac{d}{2} \cdot \tan(\phi). \tag{14}$$

In the earlier analysis, a large ϕ is preferred to ensure the clarity of contrails in images. However, when $\phi > 70°$, the $\tan(\phi)$ function increases rapidly (see Figure 3), potentially introducing significant calculation errors. Therefore, it is crucial to limit the value of ϕ to maintain the accuracy of the computations.

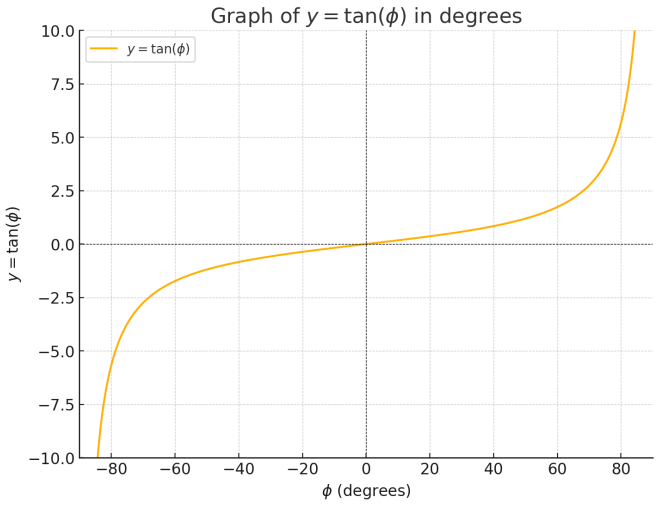

Figure 3: Graph of $\tan(\phi)$ highlighting the rapid increase for $\phi > 70°$.

In conclusion, from the analysis, we observe that increasing d leads to larger r and therefore decreases the number of pixels p representing the contrails. Conversely, reducing d requires increasing ϕ, but large values of ϕ (e.g., $\phi > 70°$) can cause significant errors in the calculation of h. Thus, an optimal balance between d and ϕ is essential to ensure accurate observation and calculation.

2.3 Approximate the GPS Coordinates of the Contrail

The objective is to approximate the GPS coordinates of the contrail using images from two cameras with known positions. The inputs required for the calculation are as follows:

- Geographic coordinates (latitude, longitude, altitude) of the two cameras are provided as (lat_1, lon_1, alt_1) and (lat_2, lon_2, alt_2).
- Camera specifications and additional data are required, including:
  - Resolution of the images (W, H).
  - Horizontal and vertical fields of view (hFOV and vFOV).
  - Tilt angle of the camera θ_{tilt}.
- Pixel coordinates of the contrail as captured by the two cameras: $((px_1, py_1), (px_2, py_2))$.

The algorithm for determining the contrail's coordinates consists of the following steps:

1. Model the problem in the $Oxyz$ coordinate system.
2. Determine the equations of the two lines connecting each camera to the contrail.
3. Find the position of the contrail as the closest point to these two lines, ideally at their intersection if there is no calculation error.
4. Compute the GPS coordinates of the contrail based on its $Oxyz$ coordinates and the GPS coordinates of one camera.

Problem Modeling

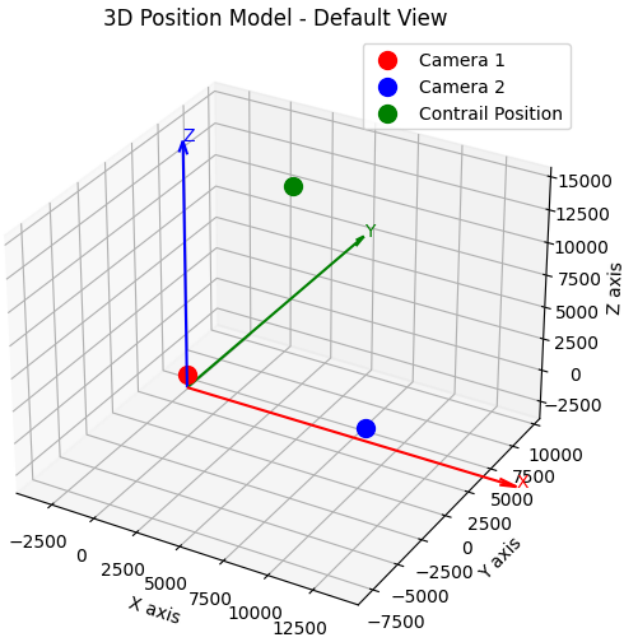

Figure 4: Modeling the problem of estimating the contrail position in the $Oxyz$ coordinate system

The problem is modeled in the $Oxyz$ coordinate system, as illustrated in Figure 4. The red point, corresponding to the origin O, represents the position of Camera 1. The Ox-axis aligns with

the line connecting the two cameras, with the position of Camera 2 represented by the blue point. The green point denotes the contrail, located at an altitude h.

The reference plane $z = 0$ coincides with the mean sea level (MSL), and altitudes are measured relative to this plane. Camera 1 is positioned at $(0, 0, alt_1)$, while Camera 2 is located at $(d, 0, alt_2)$, where d is the suggested optimal distance between the two cameras.

Determine the Equations of Camera-Contrail lines

In the $Oxyz$ coordinate system, each camera observes the contrail along a line defined by its position and direction vector. The parametric equations for these lines are expressed as:

$$L_1 : P_1 + t \cdot M_1, \quad L_2 : P_2 + s \cdot M_2, \tag{15}$$

where P_1 and P_2 represent the positions of Cameras 1 and 2, respectively, M_1 and M_2 are the corresponding direction vectors, and t and s are real-valued parameters.

The direction vectors M_1 and M_2 are derived from the horizontal angle α and the vertical angle β:

$$M_1 = \left[\sqrt{1 - \sin^2\alpha_1 - \sin^2\beta_1},\ \sin\alpha_1,\ \sin\beta_1\right], \tag{16}$$

$$M_2 = \left[-\sqrt{1 - \sin^2\alpha_2 - \sin^2\beta_2},\ -\sin\alpha_2,\ \sin\beta_2\right], \tag{17}$$

where α_1, α_2 and β_1, β_2 are the angles between L_1, L_2 and the referenced directions.

The horizontal angle α and vertical angle β are calculated as follows:

$$\alpha = -\arctan\left[\frac{(px - W/2)}{W/2} \cdot \tan(\text{hFOV}/2)\right], \tag{18}$$

$$\beta = \theta_{\text{tilt}} + \arctan\left[\frac{(py - H/2)}{H/2} \cdot \tan(\text{vFOV}/2)\right]. \tag{19}$$

Determining the Contrail's Position in the $Oxyz$ coordinate system

The values t and s for the closest points between the two lines are calculated as:

$$t = \frac{\text{dot}(\text{cross}(v, M_2), \text{cross}(M_1, M_2))}{|\text{cross}(M_1, M_2)|^2} \tag{20}$$

$$s = \frac{\text{dot}(\text{cross}(v, M_1), \text{cross}(M_1, M_2))}{|\text{cross}(M_1, M_2)|^2} \tag{21}$$

where $v = \overrightarrow{P_1P_2}$, and dot and cross represent the dot and cross products, respectively.

Finally, the estimated position of the contrail is calculated as the midpoint between the closest points:

$$(x, y, z) = \frac{(P_1 + t \cdot M_1) + (P_2 + s \cdot M_2)}{2} \tag{22}$$

Determining the Contrail's Position in the GPS coordinate system

After obtaining the results in the $Oxyz$ coordinate system, the GPS coordinates of the contrail are calculated using the GPS coordinates of Camera 1 and the following equations:

$$\text{Latitude:} \quad \text{lat}_{\text{contrail}} = \text{lat}_1 + \Delta\text{lat} \tag{23}$$

$$\text{Longitude:} \quad \text{lon}_{\text{contrail}} = \text{lon}_1 + \Delta\text{lon} \tag{24}$$

where Δlat and Δlon are the latitude and longitude offsets derived from the $Oxyz$ coordinates of the contrail and calculated using Equations 10 and 11.

2.4 Contrail Detection and Classification

The model is developed using YOLOv8n-OBB to detect and classify contrails into six categories: young contrail, old contrail, very old contrail, parasite, sun, and unknown. Classification decisions are made based on attributes such as shape, width, blur, formation time, and color.

The parasite class includes objects that resemble contrails in shape and color but do not represent actual contrails, for instance, thin clouds or smoke. The unknown class is assigned to instances with unclear identities, including image noise or unusual lighting effects. By introducing these additional classes, the model can better distinguish between contrails and non-contrails, thereby reducing classification errors.

Due to limited data availability, an open-source dataset from Roboflow (Recherdataplace, 2024) was used for training. This dataset provides images labeled with oriented bounding boxes (OBB). Figure 5 illustrates several examples from the dataset.

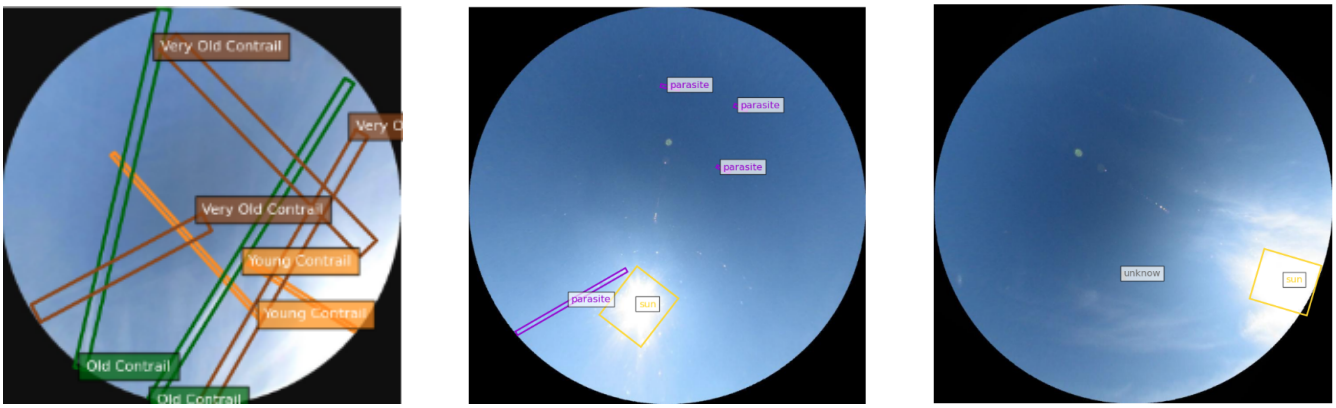

Figure 5: Samples in an open-source dataset on Roboflow

3 Results

3.1 Contrail Observation

The low-tech devices used in this project are smartphones, with main cameras featuring a focal length of 26 mm, corresponding to the 35 mm film format (commonly referred to as the full-frame format in digital photography). To calculate the field of view for these cameras, the reported focal length is treated as the *35 mm equivalent focal length*. This approach assumes the standard full-frame sensor dimensions of 36×24 mm, which serve as the reference sensor size.

The fields of view (FOV) for these cameras with a 16:9 aspect ratio are as follows:

- Horizontal FOV: 41.05°
- Vertical FOV: 67.30°
- Diagonal FOV: 74.74°

To maximize contrail observation, the first smartphone is positioned such that its central orientation θ_c is perpendicular to a specific flight path. Based on the aviation map in Figure 6, the selected flight path for observation is FL065, and therefore:

$$\theta_c = \frac{302 + 127}{2}$$

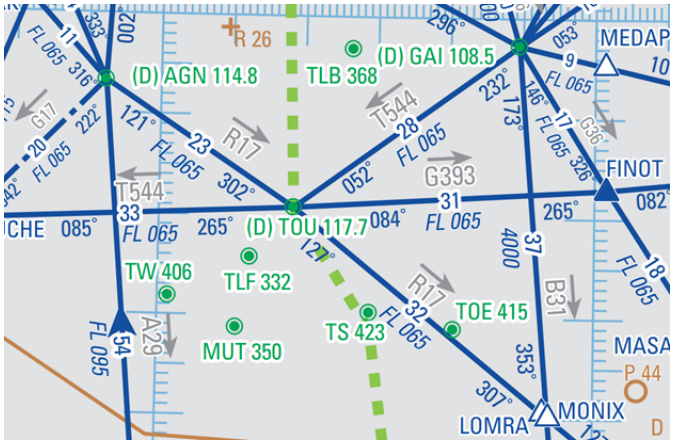

Figure 6: Aviation map of Toulouse. Image source: DIRCAM

The camera is positioned at an altitude of 16 meters above ground level, resulting in an observable distance of 14,278 m. The GPS coordinates for the current position and boundaries are provided in Table 1:

Description	Latitude	Longitude
Current GPS coordinates	43.57072605547293	1.4682620342267738
Left boundary GPS coordinates	43.44611717806291	1.425467002274119
Right boundary GPS coordinates	43.49712360251506	1.3230345133147507

Table 1: GPS coordinates for the current position and observable boundaries.

With the obtained coordinates, the observable region of Camera 1 is illustrated in Figure 7.

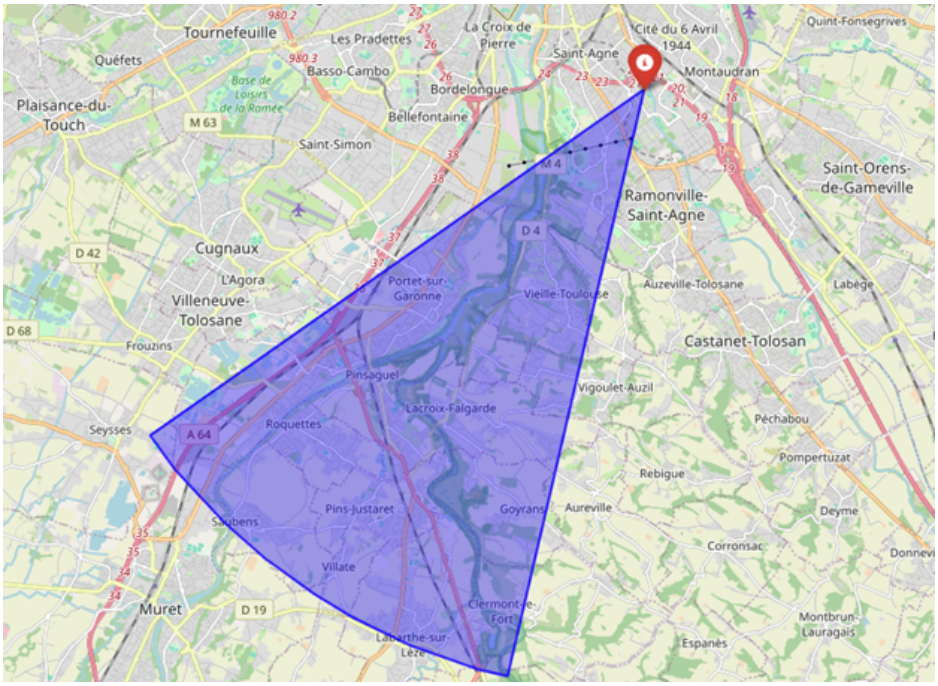

Figure 7: Observable area of the first camera

To determine the optimal position for the second camera, ϕ_1 and ϕ_2 are tested with values less than 70° to avoid significant error impact. However, the angles should not be too small, as this would increase the distance between the contrails and the cameras, reducing the number of pixels representing the contrails. Three cases are considered, with $\phi_1 = \phi_2 = \phi \in \{60°, 65°, 70°\}$. The results are shown in Table 2.

Angle ϕ	**Distance d (m)**	**Pixels p**
60°	13856	42
65°	11191	44
70°	8735	45

Table 2: Comparison of angles ϕ to select the optimal distance d based on the number of pixels p

Considering the trade-off between pixel clarity and potential error, the optimal angle $\phi = 65°$ is selected. At this angle:

- $p = 44$ pixels: sufficient for effective contrail analysis.
- ϕ is small enough to limit errors in height calculation.
- $d \approx 11,191\,\text{m}$: a reasonable distance for practical deployment.

Based on the optimal distance d determined earlier, the GPS coordinates of Camera 2 are:

$$\text{Camera 2 GPS Coordinates: } (43.487780612265304, 1.389580286057059).$$

The precise location is shown on the map in Figure 8.

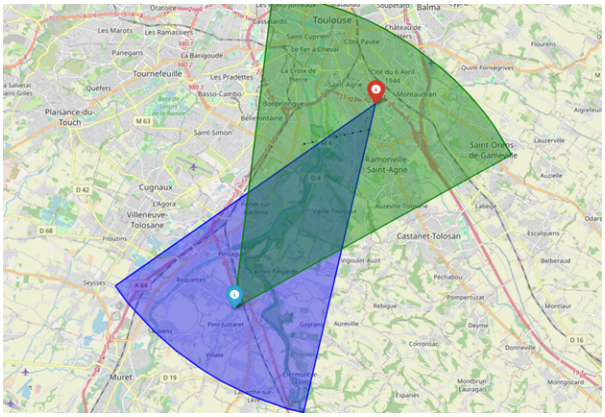

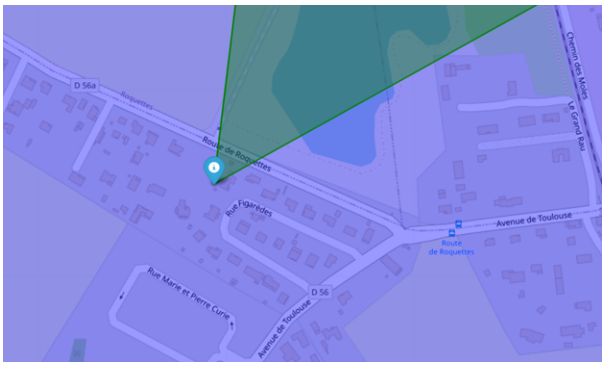

Figure 8: Proposed second camera position

3.2 Displaying the Contrail Position in $Oxyz$ and GPS

The algorithm in Section 2.3 is implemented using the previously calculated GPS coordinates and FOV of the two cameras, along with the following additional information:

- Altitude of the Cameras:
  - Camera 1: Altitude 1000 meters.
  - Camera 2: Altitude 1000 meters.
- Pixel Coordinates in the Images:
  - Camera 1: $(1020, 1160)$.
  - Camera 2: $(5040, 2320)$.
- Image Resolution:
  - Camera 1: 3840×2160 pixels.
  - Camera 2: 7680×4320 pixels.
- Tilt Angle:
  - Camera 1: $55°$.
  - Camera 2: $55°$.

The predicted coordinates of the contrail in the $Oxyz$ coordinate system are shown in Figure 9, with specific values as:

$$(5477.39, 1574.07, 10227.52).$$

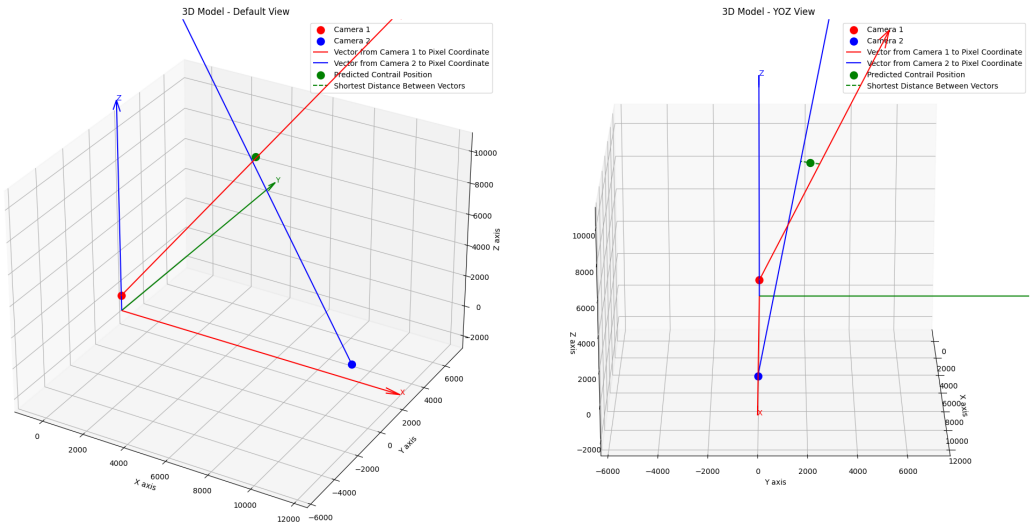

Figure 9: Contrail Prediction in Oxyz Coordinates

Based on the calculated $Oxyz$ coordinates, the geographic coordinates of the contrail are determined using Equations 10 and 11. The specific values are:

$$(43.52410463593892, 1.4388755639286046, 10227.521975806838).$$

Contrail's position is represented in both coordinate systems in Figure 10. It can be observed that the its location falls within the observable regions of both cameras.

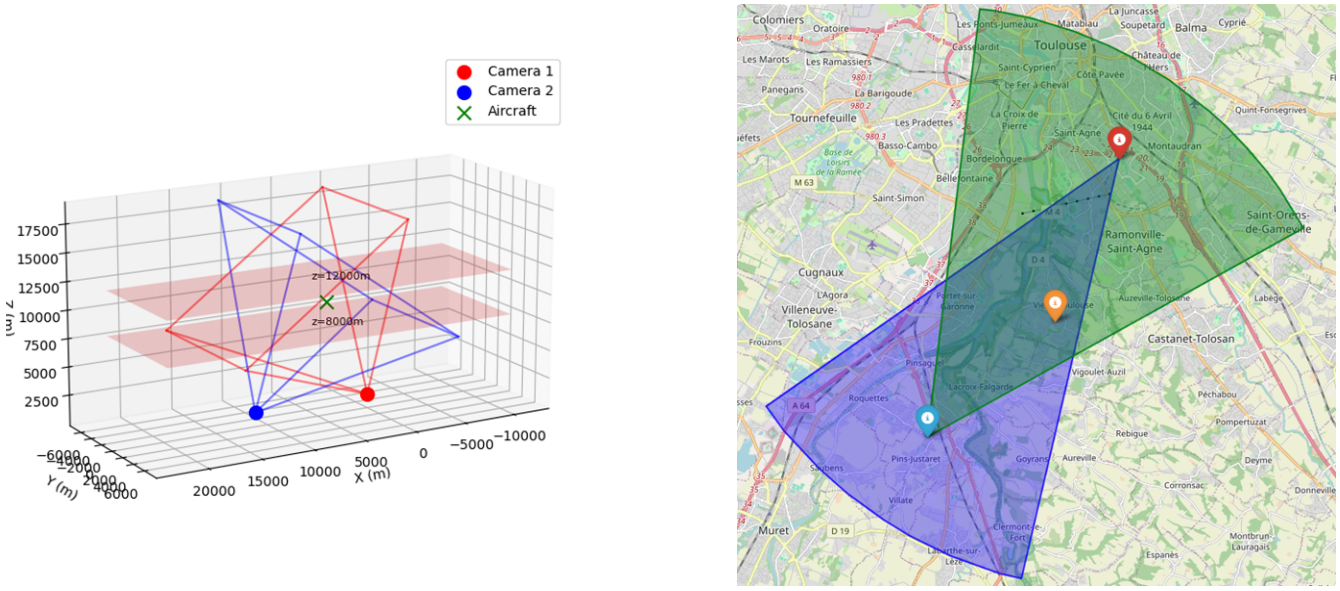

Figure 10: Contrail coordinates in $Oxyz$ and GPS systems

3.3 Contrails Detection and Classification

Evaluate model Yolov8n on validation set

Based on the evaluation results in Table 3, it can be seen that: the model shows the best performance in detecting very old contrails, with an mAP50 of 0.961, along with strong precision

Class	Images	Instances	Precision	Recall	mAP50
all	810	1789	0.858	0.833	0.896
old contrail	124	162	0.760	0.821	0.863
very old contrail	248	497	0.876	0.932	0.961
young contrail	306	388	0.803	0.631	0.759
parasite	202	323	0.866	0.762	0.883
sun	348	348	0.986	0.994	0.993
unknown	63	71	0.857	0.859	0.914

Table 3: Performance metrics for different classes.

(0.876) and recall (0.932). Old contrails demonstrate moderate performance, achieving an mAP50 of 0.863, with balanced precision (0.755) and recall (0.817). However, the model struggles most with young contrails, which have the weakest performance, with an mAP50 of 0.76 and low recall (0.631), indicating that many detections are missed.

The model's performance is challenged by young contrails, likely due to their less defined and more ambiguous features. As contrails age, their characteristics become more distinct, leading to improved detection. Very old contrails have the highest detection rates, as they are the largest and most visible, making them easier to identify. This highlights the model's strength in detecting older contrails, where their visibility is clearer.

Prediction on a test image

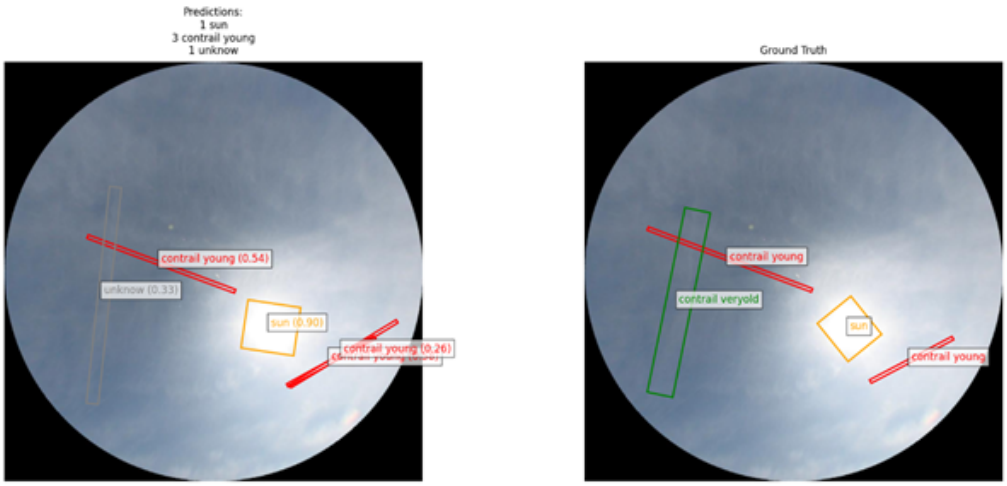

Figure 11: Visualize the prediction on the test set: Prediction (Left), Ground Truth (Right)

Figure 11 illustrates the model performs well in detecting the contrails in this image, although there is a slight misclassification where a very old contrail (in the ground truth) is mistakenly predicted as unknown. The oriented bounding boxes (OBB) are generally quite accurate.

4 Discussion

4.1 Achievements

This study has achieved some progress in the field of contrail observation and analysis:

Optimal Camera Placement

A method has been developed to determine the optimal distance between two cameras for contrail observation. By balancing factors such as contrail altitude, pixel representation, and calculation accuracy, an optimal distance of 11,191 between the camera-contrail line and the horizontal plane was proposed, ensuring effective contrail detection while minimizing potential errors in height calculations.

GPS Coordinate Calculation

An algorithm has been successfully implemented to calculate the GPS coordinates of contrails based on pixel coordinates from images captured by two fixed cameras. This method utilizes camera specifications, geographic positions, and image data to triangulate the contrail's position in 3D space. This approach enables the precise localization of contrails, which is crucial for understanding their formation and persistence.

Contrail Detection and Classification Model

A YOLOv8n-OBB model was trained on an open-source dataset for contrail detection and classification. The model achieved a good mAP-50 of 89.6% on the validation set, demonstrating its effectiveness in identifying and categorizing contrails. The model's performance varied across contrail types, with very old contrails being detected most accurately (mAP50 of 0.961) and young contrails presenting the greatest challenge (mAP50 of 0.76).

4.2 Future Directions

Several avenues for future research and improvement have been identified:

Custom Dataset Development

Currently, the model relies on existing open-source images for training and testing. A crucial next step would be to install specialized cameras at suitable locations, as determined by the calculations for optimal camera placement.

Tracking Contrail Persistence

Future research should leverage real-world footage captured by suitably placed cameras to track the persistence of contrails over time. By applying the pixel-to-coordinate algorithm in conjunction with the YOLOv8n-OBB model, the position and altitude of contrails, particularly old contrails, can be accurately determined from the captured images. This combined approach would allow for tracking the evolution and longevity of contrails in specific areas. Such temporal analysis is crucial for identifying Ice-Supersaturated Regions (ISSR), which are critical in understanding contrail formation and persistence. By mapping these ISSR zones, valuable data for aviation route

planning could be provided, contributing to more effective strategies for mitigating the climate impact of aviation.

Aircraft Type Matching

An important next step would be to develop methods for matching observed contrails with their corresponding aircraft types. This could involve integrating real-time flight data with the contrail detection system. By correlating contrail characteristics with specific aircraft models, insights could be gained into how different aircraft contribute to contrail formation.

5 Conclusion

This research presents a comprehensive framework for ground-based contrail observation and analysis, addressing the growing concern about aviation's non-CO2 emissions. The study introduces a detailed methodology for determining camera coverage areas and their optimal placement. This methodology considers factors such as the field of view, maximum observable distance, and boundary coordinate calculations. By incorporating these factors, the proposed approach ensures efficient and accurate contrail monitoring over large areas.

An analysis of the optimal distance between two cameras is also presented, aiming to balance the trade-offs between image clarity and calculation accuracy. The study recommends a setup with an approximate 11 km distance between cameras, which provides a practical compromise for effective deployment. Additionally, an algorithm has been developed for approximating contrail GPS coordinates using data collected from two ground-based cameras. This algorithm is useful for tracking flights responsible for producing contrails.

To further support contrail monitoring, a YOLOv8n-OBB model has been implemented for contrail detection and classification. The model is capable of distinguishing between young, old, and very old contrails, as well as identifying potential false positives. However, the YOLO model was trained using an open-source dataset available on Roboflow, rather than real-world data captured by ground-based cameras. The model demonstrates promising performance, particularly for detecting older and more defined contrails.

The study has yet to incorporate real-world data collected from ground-based cameras for validation. Future work could apply the proposed methods and models to identify contrails in images, as well as their coordinates and altitudes. This information could contribute to identifying Ice-Supersaturated Regions (ISSR) and identify the type of aircraft responsible for long-lasting contrails that impact Earth's temperature.

References

FAA. (2000). Aircraft contrails factsheet [EPA430-F-00-005, September 2000]. https://www.faa.gov/sites/faa.gov/files/regulations_policies/policy_guidance/envir_policy/contrails.pdf

Knight, D. W. (2018). *Lens field of view* [Updated Feb. 2018. David Knight asserts the right to be recognised as the author of this work.]. https://www.g3ynh.info/photography/articles/Lens_fov.html

Lee, D. S., Fahey, D. W., Skowron, A., Allen, M. R., Burkhardt, U., Chen, Q., Doherty, S. J., Freeman, S., Forster, P. M., Fuglestvedt, J., et al. (2021). The contribution of global aviation to anthropogenic climate forcing for 2000 to 2018. *Atmospheric environment*, *244*, 117834.

Recherdataplace. (2024, February). Contrails dataset [visited on 2025-01-22]. https://universe.roboflow.com/recherdataplace/contrails-0lwhn